A Study on the Preparation and Optical Properties of Semiconductor Nanoparticles of ZnO, ZnS and $ZnS:Mn^{2+}$

ZnO, ZnS, $ZnS:Mn^{2+}$ 반도체 나노입자들의 합성과 광학적 특성에 관한 연구

A thesis submitted in partial fulfillment of the requirements.

for the degree of

Master of Science

in the Departement of Chemistry, Graduate School,

Pukyong National University

February 2004

A Study on the Preparation and Optical properties of Semiconductor Nanoparticles of ZnO, ZnS and ZnS:Mn^{2+}

A Dissertation

by

Ho-Ju Jeon

Approved as to style and content by :

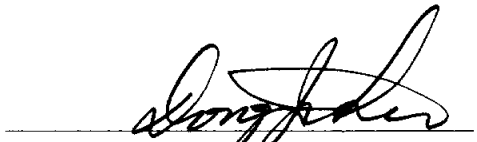

Chair man : Dong Jae Lee

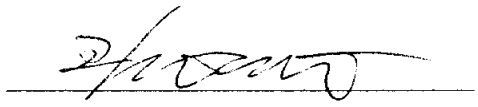

Member : Sung Doo Moon

Member : Young Soo Kang

December 2003

Contents

List of Figures

List of Table

Study on the Preparation and the Optical Properties of Semiconductor Nanoparticles of ZnO, ZnS and ZnS:Mn^{2+}

Ho-Ju Jeon

Department of Chemistry, Graduate School
PuKyong National University

Abstract

ZnO and ZnS is a wide-band gap II ~ VI semiconductor and might be a good candidate for a short wavelength optoelectronic device. ZnO nanopaticles were prepared by addition of LiOH to an ethanolic zinc acetate solution. The synthesis of ZnO was done by hydrolysis using sol-gel method. ZnO nanoparticle was controlled by heat-treatment. ZnS and manganese doped ZnS (ZnS:Mn^{2+}) nanocrystals were prepared by adding Na_2S to the solutions of zinc oleate and zinc oleate mixed with $Mn(NO_3)_2$. It was performed by thermal decomposition using auto-clave method. The aging of the complexes in auto-clave resulted in ZnS and Mn^{2+} doped ZnS nanoparticles. The optical properties of ZnO nanoparticles greatly depend on the particle size and those of ZnS:Mn^{2+} depend on the amount of added Mn^{2+}. The size of ZnO nanoparticles was determined by TEM images, XRD line widths and UV-vis spectra. The amount of Mn^{2+} was determined by TEM- EDX.

1. Introduction

Research on nanocrystalline materials has increased enormously during past years. Semiconductor nanoparticle with dimensions smaller than or in the order of the size of bulk exciton show unique optical properties, which depend strongly on the size. These properties have stimulated great interest in semiconductor nanoparticles both from a fundamental and from an applied point of view. The change of the energy level structure can be explained by strong confinement of the charge carriers in all three dimensions. Besides the size quantization, surface effects can strongly influence the optical properties of these nanoparticles. Optical properties of semiconductor nanocrystallines have been investigated, since these materials have a potential application to nonlinear optical devices. The luminescence properties of nanosized luminescent semiconductor particles are substantially different from those of bulk crystalline materials. The band gap energy increases as particles become a small, such small particles emit visible luminescence intensity much stronger than bulk crystals. ZnO and ZnS is a wide-band gap II ~ VI semiconductor and might be a good candidate for a short wavelength optoelectronic device

Zinc oxide (ZnO) have a band gap of 3.37 eV at room temparature and

emit identically at UV range as direct semiconductor.[1] In general, ZnO have a hexagonal wurtzite structure (a = 3.14 Å, c = 5.21 Å).[2] Since ZnO nanoparticles generally have property of n-type semiconductor due to lack of oxygen or excess of zinc, the ZnO nanoparticles emit at the visible range of green and yellow.[3] In this paper, ZnO nanoparticles have been prepared by sol-gel method. We have synthesized ZnO colloids by changing annealing temperature and time to get optimum condition for the optical properties of ZnO nanoparticles, because it depends on the particle size. ZnO has been considered as a promising material for devices such as piezoelectric transducer, optical waveguide and solar cell.[4]

Also, zinc sulfide (ZnS) is semicondutor material with an energy band gap of 3.6 eV.[5] Since the effective energy band gap is 339 nm at room temperature with its energy band characteristic, ZnS becomes a good host material. ZnS is particularly suitable for use as a host material for a large variety of dopants because of its wide energy band gap. In addition, the luminescent properties of this material doped with Mn have proven to be adequate for electroluminescent applications.[6] The manganese usually occupies substitutionally the Zn lattice sites as a divalent ion, and the excitation and decay of this ion produces a yellow luminescence at approximately 585 nm. Bhagrava et al.[7] have reported that the

luminescence enhancement of manganese doped ZnS ($ZnS:Mn^{2+}$) results from an efficient energy transfer from the ZnS host to Mn^{2+} ions facilitated by mixed electronic states. The hybridization of atomic orbital of ZnS and d orbital of Mn^{2+} was also suggested to be responsible for the relaxation of selection rules for the spin-forbidden $^4T_1$-$^6A_1$ transition of Mn^{2+}. In this paper, we report the preparation and optical properties of Mn^{2+} doped ZnS semiconductor. The synthesis of $ZnS:Mn^{2+}$ was done by thermal treatment oleate complexes of them using auto-clave. The aging of zinc oleate and manganese doped zinc oleate in auto-clave resulted in $ZnS:Mn^{2+}$ nanoparticles.

2. Experimental

2-1. Materials

Zinc acetate dihydrate ($C_4H_6O_4Zn{\cdot}2H_2O$), lithium hydroxide monohydrate ($LiOH{\cdot}H_2O$), Manganese (II) nitrate hydrate ($Mn(NO_3)_2$, 98%) and sodium sulfide (Na_2S, absolute) were purchased from Aldrich Chemical Company Inc. Zinc chloride ($ZnCl_2$, extra pure) and sodium oleate ($C_{17}H_{33}COONa$, extra pure) were purchased from Junsei Chemical Co., Ltd. Ethanol as solvent was used without any further purification

2-2. Apparatus

The size of ZnO, ZnS and ZnS:Mn^{2+} nanoparticles was determined with Transmission Electron Microscope (TEM) (JEOL, JEM-2010) and analysis of the line width of the X-ray diffraction (XRD) (Philips, X'Pert-MPD system). TEM samples were prepared on the 400 mesh copper grid coated with carbon. A drop of the nanoparticle solution was placed on the copper grid and dried in air. The size distribution of the particles was determined from the enlarged photographs of TEM image. The average size of the crystals was also estimated with XRD spectrum using Debye-Scherrer equation. The crystal structure was studied with XRD. And analysis of element was confirmed by TEM - Energy dispersive X-ray (TEM-EDX). The emission spectra were recorded on a Luminescence Spectrometer (Perkin-Elmer, LS50B) and the absorption spectra were on UV-vis spectrometer (Varian, Cary 1C).

2-3. Methods

2-3-1. Preparation of ZnO nanoparticles

Preparation of ZnO nanoparticle involves three steps using sol-gel method.[8][9] : (1) preparation of organometallic precursor containing 0.1 M Zn, (2) preparation of ZnO colloids, (3) solvent removal by rotary evaporation to the concentration levels resulting in desired products such as

syrups and gels and (4) annealing at 300 ^{0}C for crystallization and removing acetate

(1) Organometallic Zn precursor

A 50 mL of ethanol containing zinc acetate (1.0975 g, 5 mmol) was placed into a distillation apparatus (Figure 1) fitted so that the reaction can be done under atmospheric pressure, avoid moisture exposure, and collect condensate. Over a period of 3 hours, the solution was boiled at 80 ^{0}C and stirred with a magnetic stirring bar. At the end of this procedure, 30 mL of condensate and 20 mL of hygroscopic reaction mixture were obtained. The hygroscopic product was diluted to maintain 0.1 M ethanolic solution containing the zinc acetate.

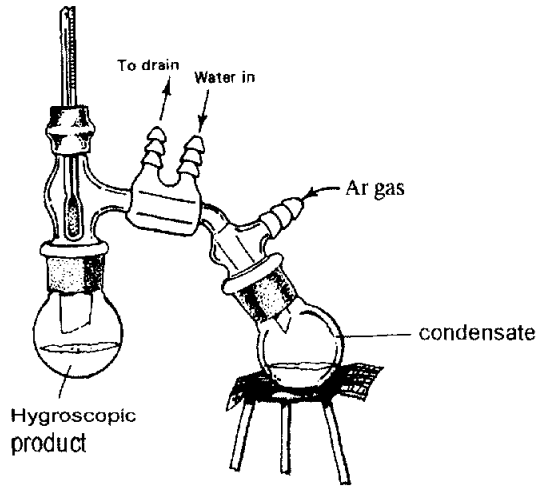

Figure 1. Distillation apparatus for the prepared organometallic Zn precursor

(2) ZnO colloids

ZnO colloid was synthesized by addition of lithium hydroxide monohydrate (0.05245 g, 1.25 mmol) to the ethanolic solution. Finally, the suspension was placed into an ultrasonic bath in order to destroy the weakly soluble powder. This procedure accelerates the release of OH^- ions, resulting in immediate reaction to form a stable ZnO cluster solution. The nucleation reaction can be written as [10]

$$Zn(CH_3CO_2)_2 + LiOH \rightarrow ZnO + H_2O + LiCH_3CO_2$$

This reaction is performed at 0 ^{0}C and under air conditions for 10 min. Room temperature preparation give slightly larger particles.

(3) Crystal growth

Crystal growth is, in most cases, a self-induced process occurring at room temperature. For the crystallization of ZnO nanoparticle, the synthesized ZnO colloid was treated by heating under the several conditions. ; Among the non-treated ZnO colloid, fresh colloid is ZnO I and 6-month-old colloid is ZnO II. ZnO colloid was refluxed for 12 hours (ZnO III) and 120 hours (ZnO IV). Finally, ZnO particles prepared by evaporation were annealed at 300 ℃ for 2 hours (ZnO V). Solvents of ZnO I, II, III and IV colloids were

removed by rotary evaporation.

2-2-2. Preparation of ZnS and ZnS:Mn^{2+} nanoparticles

ZnS and ZnS: Mn^{2+} nanoparticles were prepared by auto-clave method. ZnS was synthesized as follows: A 2.23 g (7.34 mmol) of sodium oleate was dissolved in 100 ml of water. And it was added the sodium oleate solution to 0.5 g (0.0367 mol) of zinc chloride and 0.285 g (3.65 mmol) of Na_2S under constant stirring for 2 hours. The mixture was slowly heated from room temperature to 300 °C at 60 °C/30 min. After reaching the desired temperature, it was held at 300 °C for 2.5 hours and cooled to room temperature. The color of product was gray. The reaction product was diluted to methanol and filtered through membrane filter (0.45 μm). The synthetic method of ZnS:Mn^{2+} nanoparticle was similar to that of ZnS nanoparticles. Before the addition of Na_2S, a desired amount of $Mn(NO_3)_2$ and sodium oleate was added to zinc oleate solution. The next process was the same with that of ZnS nanoparticles. ZnS:Mn^{2+} nanoparticles was prepared by various concentration of $Mn(NO_3)_2$; ZnS:Mn^{2+} I nanoparticles was synthesized by 0.0367 mol $Mn(NO_3)_2$, ZnS:Mn^{2+} II nanoparticles was synthesized by 0.0257 mol $Mn(NO_3)_2$, ZnS:Mn^{2+} III nanoparticles was synthesized by 0.0184 mol $Mn(NO_3)_2$.

3. Background

(1) Sol-gel method :

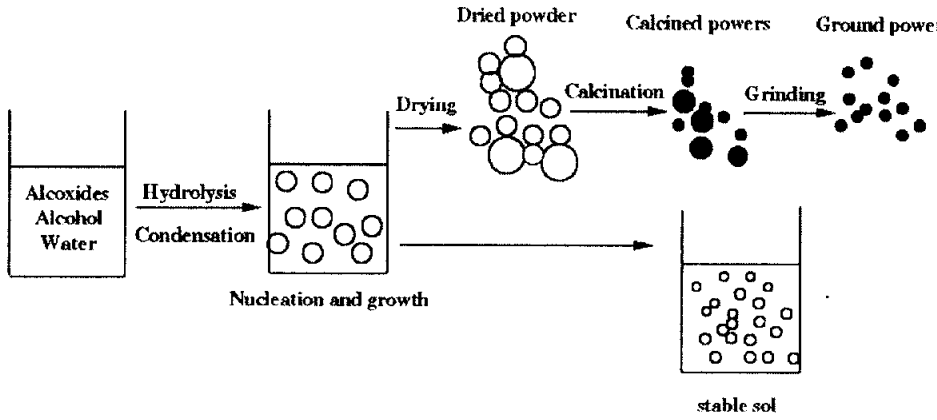

Figure 2. Overview of the sol-gel process

Among the synthetic method of nanoparticles, sol-gel processing is a wet chemical synthetic method by gelation, precipitation and hydrothermal treatment. Also, the process (Figure 2) has been known as preparation of metal oxide.[11][12][13][14] The colloid is a suspension in which the dispersed phase is so small (1 ~ 1000 nm) that gravitational forces are negligible and interactions are dominated by short-range forces, such as Van der Waals attraction and surface charges. The inertia of the dispersed phase is small enough that it exhibits Brownian motion (or Brownian diffusion), a random walk driven by momentum imparted by collisions with molecules of the

suspending medium. A sol is a colloidal suspension of particles in a gas (the suspension may be called a fog if the particles are liquid and a smoke if they are solid) and droplets in another liquid. All of these types of colloids can be used to generate polymers or particles from which ceramic materials can be made. A ceramic is usually defined by saying what it is not: it is nonmetallic and inorganic. In the sol-gel process, the precursors (starting compounds) for preparations of a colloid consist of a metal or metalloid element surrounded by various ligands (appendages not including another metal or metalloid atom). For example, common precursors for aluminum oxide include inorganic (containing no carbon) salts such as $Al(NO_3)_3$ and organic compounds such as $Al(OC_4H_9)_3$. The latter is an example of an alkoxide, the class of precursors most widely used in sol-gel research. An alkane is a molecule containing only carbon and hydrogen linked exclusively by single bonds, as in methane (CH_4) and ethane (C_2H_6); the general formula is C_nH_{2n+2}. An alkyl is a ligand formed by removing hydrogen (proton) from an alkane molecule producing, for example, methyl ($-CH_3$) or ethyl ($-C_2H_5$). An alcohol is a molecule formed by adding a hydroxyl (OH) group to an alkyl (or other) molecule, as in methanol (CH_3OH) or ethanol (C_2H_5OH). An alkoxy is a ligand formed by removing a proton from the hydroxyl on an alcohol, as in methoxy ($-OCH_3$) or ethoxy ($-OC_2H_5$).

Metal alkoxides are members of the family of metalorganic compounds, which have an organic ligand attached to a metal or metalloid atom. The most throughly studied example is silicon tatraethoxide (or tetraethoxysilane, or tetraethyl orthosilicate, TEOS), $Si(OC_2H_5)_4$. Organometallic compounds are defined as having direct metal-carbon bonds, not metal-oxygen-carbon linkages as in metal alkoxides; thus, alkoxides are not organometallic compounds, although that usage turns up frequently in the literature. Metal alkoxides are popular precursors because they react readily with water. The reaction is called hydrolysis, because a hydroxyl ion becomes attached to the metal atom, as in the follow reaction:

$$Si\ (OR)_4 + H_2O \rightarrow HO\text{-}Si\ (OR)_3 + ROH$$

The R represents a proton or other ligand (if R is an alkoxy group), and ROH is an alcohol. Depending on the amount of water and catalyst present, hydrolysis may go to completion (so that all of the OR groups are replaced by OH), or stop while the metal is only partially hydrolyzed, $Si(OR)_{4-n}(OH)_n$.

$$Si(OR)_4 + 4H_2O \rightarrow Si(OH_4) + 4ROH$$

Inorganic precursors can be hydrolyzed. Two partially hydrolyzed molecules can link together in a condensation reaction, such as

$$(OR)_3Si\text{-}OH + HO\text{-}Si(OR)_3 \rightarrow (OR)_3Si\text{-}O\text{-}Si(OR)_3 + H_2O$$

or

$$(OR)_3Si\text{-}OR + HO\text{-}Si(OR)_3 \rightarrow (OR)_3Si\text{-}O\text{-}Si(OR)_3 + ROH$$

By definition, condensation liberates a molecule, such as water or alcohol. This type of reaction can continue to build larger and larger silicon containing molecules by the process of polymerization.

If a monomer can make more than two bonds, then there is no limit on the size of the molecule that can form. If one molecule reaches macroscopic dimensions so that it extends throughout the solution, the substance is said to be a gel. Thus a gel is a substance that contains a continuous solid skeleton enclosing a continuous liquid phase. The continuity of the solid structure gives elasticity to the gel (as in familiar gelatin desert). Gels can also be formed from particulate sols, when attractive dispersion forces cause them to stick together in such a way as to form a network. Gelation can occur after a sol is cast into a mold, in which case it is possible to make objects of a desired shape. If the smallest dimension of the gel is greater

than a few millimeters, the object is generally called a monolith. Alternatively, gelation can be produced by rapid evaporation of the solvent, as occurs during preparation of films or fibers.

Drying by evaporation under normal conditions gives rise to capillary pressure that causes shrinkage of the gel network. The resulting dried gel, called a xerogel (xero means dry), is often reduced in volume by a factor of 5 to 10 compared to the original wet gel. If the wet gel is placed in an autoclave and dried under supercritical conditions, there is no interface between liquid and vapor, so there is no capillary pressure and relatively little shrinkage. The process is called supercritical (or hypercritical) drying, and the product is called an aerogel. These may indeed be mostly air, having volume fractions of solid as low as ~1%. Xerogel and aerogels area useful in the preparation of dense ceramics, but they are also interesting in themselves, because their high porosity and surface area make them useful as catalytic substrates, filters, and so on.

(2) Quantum size effect

Quantum size effect in semiconductor nanoparticles have been as subject of extensive studies in recent year. The size quantization effect is most directly detected as the energy shift (blue shift) of the absorption or the

luminescence peak in these materials. The theoretical band gap shift (ΔE) based on the effective mass approximation is defined as

$$\Delta E = \frac{h^2 \pi^2}{2r^2}\left(\frac{1}{m_e} + \frac{1}{m_h}\right) - \frac{1.786\, e^2}{\varepsilon\, r} - \frac{0.248\, e^4}{2\varepsilon^2 h^2}\left(\frac{1}{m_e^{-1} + m_h^{-1}}\right)$$

where, r is nanoparticle radius, ε is the dielectric constant. m_e and m_h are effective mass of the electron and hole respectively.

(3) Luminescence

Luminescence is the phenomenon of emission of electromagnetic radiation. Luminescence emission involves radiative transitions between electronic energy levels of the material, and the emission is characteristic of the material. The transition originates on some excited electronic level, and after the emission of photon a lower electronic level is occupied. The general phenomena of luminescence have been also classified into two items according to the duration of the emission following removal of excitation. If the excitation and emission process occurs in times approximating the natural lifetime of excited non-metastable isolated atom, the process is called as fluorescence. While longer duration processes are called phosphorescence. Phosphorescence involves temporary storage of potential luminescence energy, for example, of trapped excited electron, or electrons

in metastable states. Figure 3 shows the electronic absorption and emission in a diatomic molecule. Figure 4 shows radiation mechanism in semiconductors.

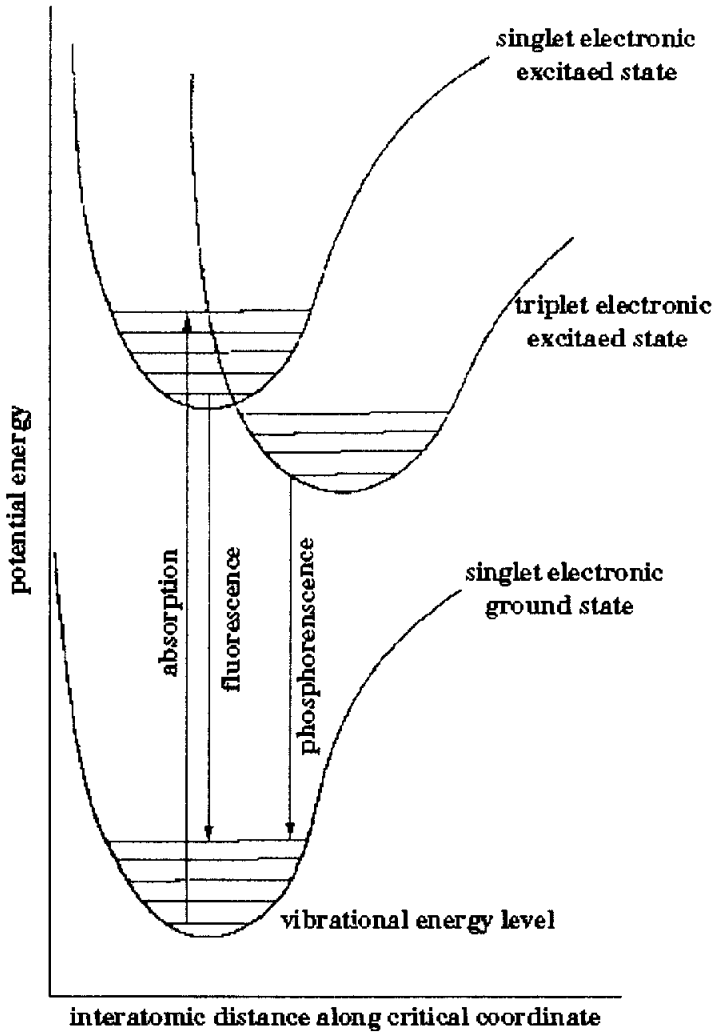

Figure 3. The electronic absorption and emission in a diatomic molecule

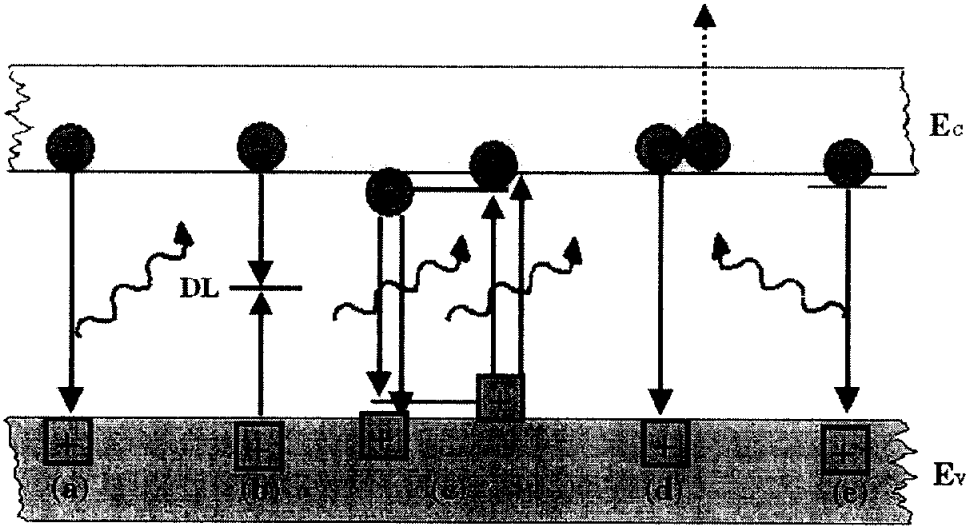

Figure 4. Radiation mechanism in semiconductors ; (a) band to band recombination, (b) recombination via deep level, (c) donor-acceptor recombination, (d) Auger recombination, (e) exiton recombination,

4. Results and Discussion

4-1. Characterization of ZnO nanoparticle

4-1-1. The structure and particle size of the ZnO nanoparticle

ZnO nanoparticles were synthesized successfully by sol-gel method and the crystal structure was confirmed by XRD patterns as Figure 5. The discernible peak in Figure 5 can be indexed to (100), (002), (101), (102), (103), and (112) plane, which corresponds to that of wurtzite structure of ZnO (JCPDS card no. 05-0664). As increasing heating time and temperature of ZnO colloid, diffraction peaks were more intense and narrower. It means that ZnO nanoparticles were crystallized by heat treatment.

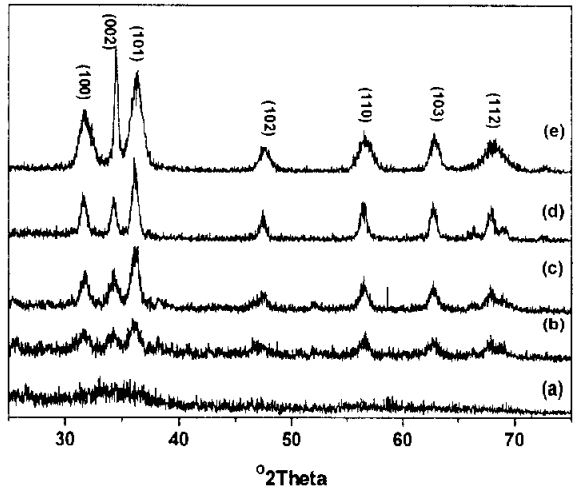

Figure 5. X-ray diffractograms of ZnO powders : (a) ZnO I, (b) ZnO II, (c) ZnO III, (d) ZnO IV, and (e) ZnO V

The crystallite size of a powder sample can be estimated from the X-ray diffraction spectrum line broadening by using the well-known Scherrer-Warren equation.

$$L = \frac{0.89 \times \lambda}{B(2\theta) \times \cos\theta}$$

Where B(2θ) is the line width of the X-ray pattern at half peak-height in radians, λ is the wavelength of the X-ray (1.54056 Å for the Cu K1α), θ is the angle between incident and diffracted beams in degrees, and L is the crystallite size of the powder samples in angstroms.

The size of ZnO I nanoparticle could not be measured by XRD because ZnO I nanoparticle is amorphous. θ values and line widths of ZnO II, ZnO III, ZnO IV and ZnO V nanoparticles were indicated in the Table 1. The results of calculated diameter of ZnO II, III, IV and V nanoparticles from XRD spectrum are 8.976, 9.526, 12.776, and 7.41 nm, respectively.

Table 1. The θ values and line widths of ZnO nanoparticle samples

sample	θ	B(2θ)
ZnO II	36.18165	0.9207
ZnO III	35.95360	0.8670
ZnO IV	36.20102	0.6467
ZnO V	36.38786	1.1156

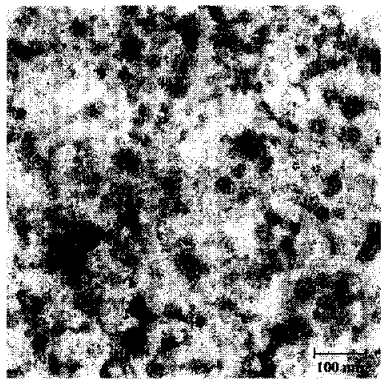

(a) ZnO I

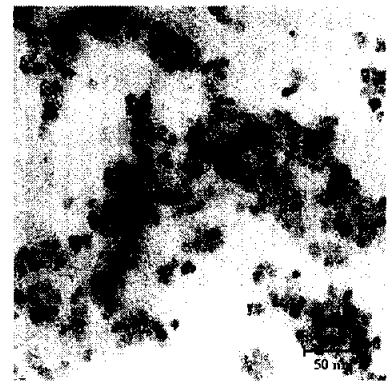

(b) ZnO II

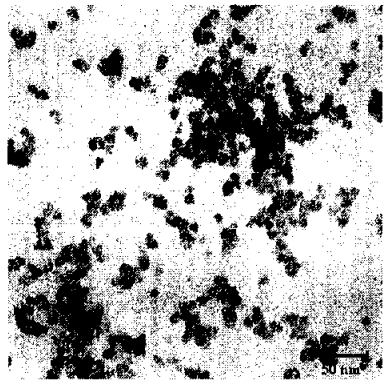

(c) ZnO III

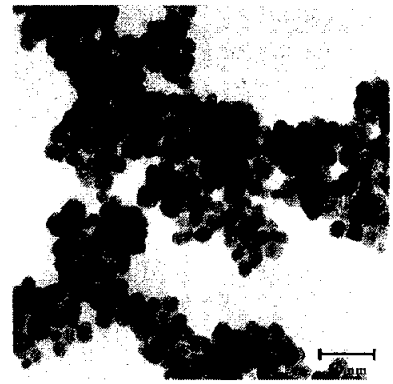

(d) ZnO IV

(e) ZnO V

Figure 6. Transmission electron microscopic images of ZnO nanoparicles

The nanoparticles of ZnO samples were depicted in the TEM images of Figure 6. ZnO nanoparicles can be easily redispersed in ethanol. TEM samples were prepared on the 400 mesh copper grid coated with carbon. ZnO nanoparticle in ethanol solution was carefully placed on the copper grid and dried in the air. Most of the ZnO nanoparticles with the exception of ZnO V are spherical. Since ZnO I nanoparticles is amorphous and the size is so small, the nanoparticle was identified clearly from Figure 6 (a). The size of ZnO I nanoparticle is estimated as approximately ~3.5 nm. And diameters of ZnO II, ZnO III, and ZnO IV are about 7.9 nm, 10.5 nm, and 15.8 nm, respectively. They have spherical shape. Unlike other ZnO samples, ZnO V nanoparticle annealed at 300 ^{0}C is needle-shaped. The length is 34.9 nm and thickness is about 5.5 nm.

The XRD data (Figure 5. (e)) shows that the (002) plane of ZnO V nanoparticles has sharpened up which is consistent with rod formation along the c axis. Caludia et al have referred that the reason is caused by the wurtzite structure itself. If complete (002) planes are formed, their reactivity should be different of the c axis from the top of the c axis. Zn and O atoms are located in an alternating manner in the (100) planes parallel to the c axis (Figure 7). Thus, hydroxylation and counter ion adsorption should be different. Different amounts of counter ions or different surface charges

could suppress or favor oriented attachment which requires an intimate contact of the respective surface planes. Also the acetate ions from the precursor salt might act in this sense. [15]

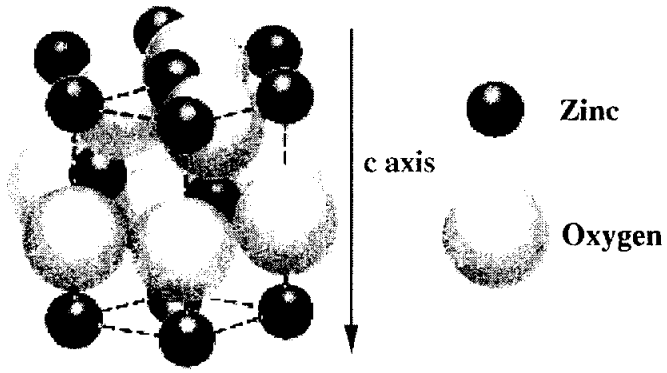

Figure 7. Wurtzite structure of ZnO

4-1-2. Optical property of ZnO nanoparticle

The UV-vis spectra of ZnO I ~ V nanoparticles are shown in Figure 8. ZnO nanoparticles have been shown to present a quantum size effect. That is, the absorption shifts to blue with decreasing crystalline size when the size is sufficiently small. ; The absorption bands of ZnO I, ZnO II, ZnO III, ZnO IV, and ZnO V nanoparticles are 304, 340, 350, 357, and 365 nm, respectively.

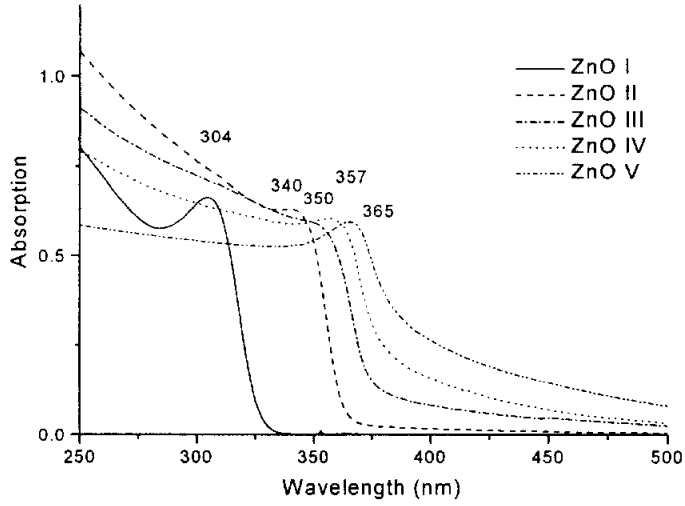

Figure 8. UV-Vis absorption spectra of ZnO I, ZnO II, ZnO III, ZnO IV, and ZnO V nanoparticles in ethanol

The photoluminescence emission spectra of ZnO I, ZnO II, ZnO III, and ZnO IV nanoparticles are shown in Figure 9. ZnO I ~ IV nanoparticles showed an emission band at 527, 536, 544, and 554 nm, respectively. The red-shift of emission peak also resulted from particle size. The width of the emission peaks of ZnO nanoparticles narrow more and more as heating time increases. This means that the particles become homogeneous size by increased heating temperature.

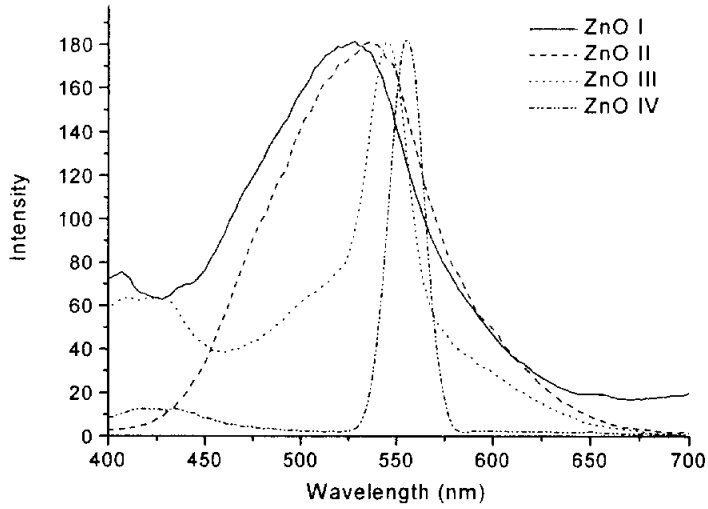

Figure 9. The emission spectra of ZnO I, ZnO II, ZnO III, and ZnO IV nanoparticles

Unlike other ZnO nanoparticles, ZnO V nanoparticle did not emit at 500 ~ 600 nm, which results from the crystal structure of ZnO V nanoparticle as shown in Figure 4(e). Usually stoichiometric ZnO shows strong UV light luminescence in the range of 370 ~ 390 nm at room temperature. Because the ZnO nanoparticles have n-type semiconductor properties, ZnO nanoparicles with the exception of ZnO V emit at visible range. The wurtzite structure of ZnO nanoparticle contains large voids which can easily accommodate interstitial atoms because of the large size of the oxygen ions as shown in Figure 7.[16] So it is virtually impossible to prepare really pure

crystals.[17] In the crystal, oxygen exists in the form of O^{2-} ions. But, it escapes as neutral O atom (O_2 gas). Consequently each escaping oxygen atom leaves two electrons behind. There are three ways in which these excess electrons can be accommodated in the crystal. One possibility is that both electrons combine with a Zn^{2+} ion to form a neutral atom. It means that the conduction electrons come from initially neutral zinc atoms. Alternatively, one or both of the electrons may occupy empty quantum states in the conduction band of the crystal and lead an existence that is essentially divorced from the zinc atoms. This can be happened in two ways. The excess zinc atoms enter interstitial sites in the crystal. The increased conductivity of the crystals implies that these zinc atoms are not electrically neutral. As these reasons, ZnO have an n-type character. Consequently, ZnO usually shows visible light luminescence due to defect related deep level emissions, such as Zn interstitials or oxygen vacancies.[18]~[24] However, the detailed luminescence center of the ZnO has not been reported. Figure 10 shows the luminescence mechanism of ZnO. The arrow (1) represents 'band to band recombination' which resulted in the emission of UV light. The arrow (2) is a green-yellow emission.[25][26][27]

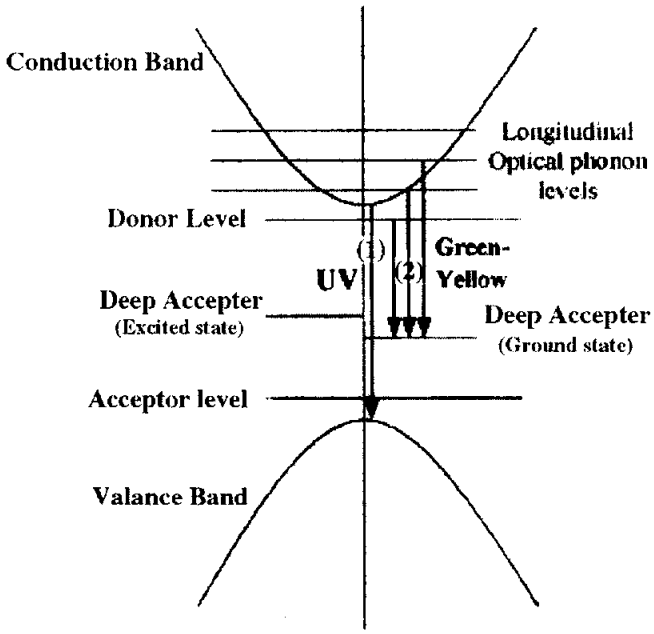

Figure 10. Luminescence mechanism of ZnO nanoparticle

4-2. Characterization of ZnS and ZnS:Mn^{2+} nanoparticles

4-2-1. The structure and particle size determination of ZnS and ZnS:Mn^{2+} nanoparticles

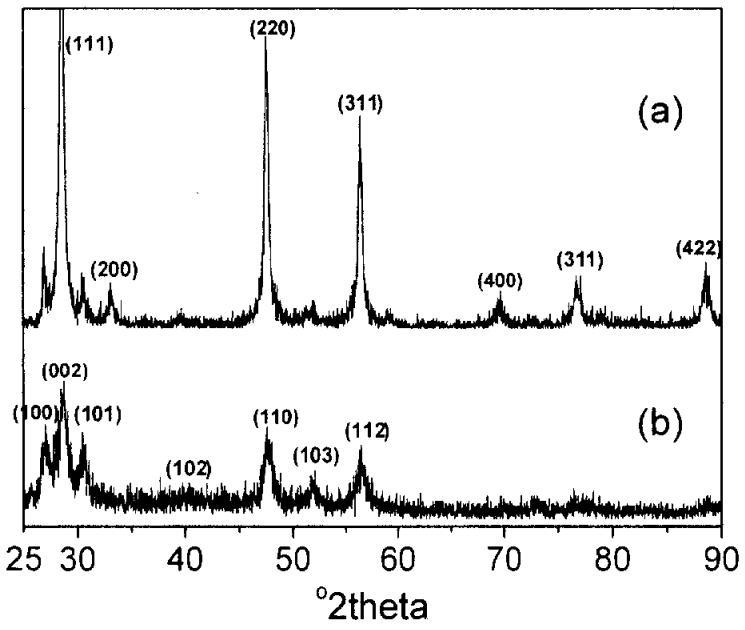

Figure 11. X-ray diffraction patterns of ZnS (a) and ZnS:Mn^{2+} (b) nanoparticles

ZnS and ZnS:Mn^{2+} nanoparticles were synthesized successfully by thermal decomposition of zinc oleate and manganese doped zinc oleate complex using auto-clave and their crystal structures are confirmed by XRD patterns as Figure 11. The discernible peak in Figure 11 (a) can be indexed

to (111), (200), (220), (311), (400), (311) and (422) planes, which corresponds to that of sphalerite structure of ZnS (JCPDS card no. 01-0792), and the discernible peaks in Figure 11 (b) can be indexed to (100), (002), (101), (102), (110), (103) and (112) planes, which correspond to that of wurtzite structure of ZnS (JCPDS card no. 75-1534).

The nanoparticles of ZnS and ZnS:Mn^{2+} were depicted in the TEM images of Figure 12 and 13. Since we synthesized ZnS and ZnS:Mn^{2+} nanoparticles at violent conditions by auto-clave method, the particle size was not regular. The diameter was determined as 8 ~ 13 nm from the TEM images. Since the particle is surrounded with oleate as capping surfactant, ZnS and ZnS:Mn^{2+} nanoparticles have an excellent monodisperse state.

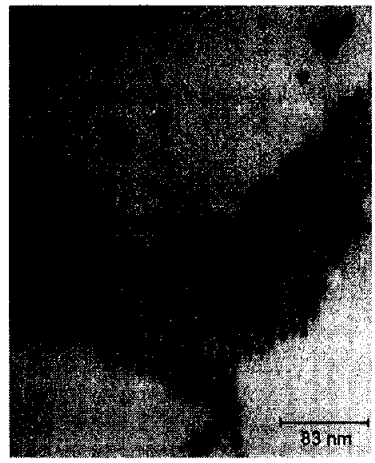

Figure 12. Transmission electron microscopic image of ZnS nanoparticles

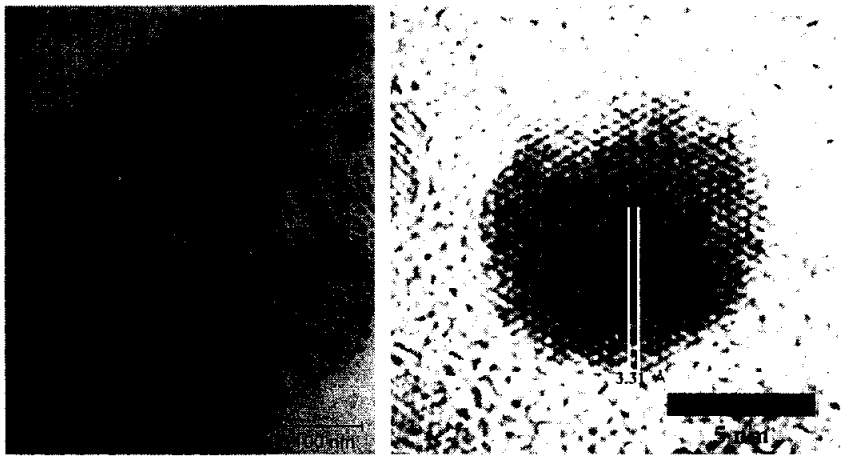

Figure 13. Transmission electron microscopic images of ZnS:Mn^{2+} nanoparticles

4-2-2. Optical properties of ZnS and ZnS:Mn^{2+} nanoparticles

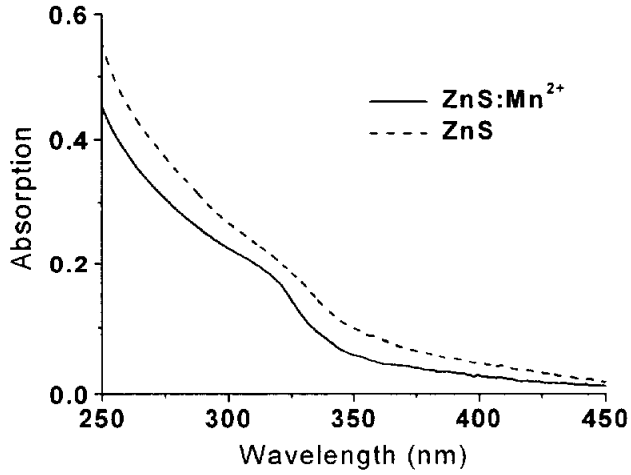

Figure 14. UV-vis spectra of ZnS and ZnS:Mn^{2+} nanoparticles

The absorption spectra of ZnS and ZnS:Mn^{2+} nanoparticles are shown in Figure 14. ZnS and ZnS:Mn^{2+} nanoparticles showed optical absorption band at $\lambda_{abs.}$ = 319 nm. Figure 15 is emission spectra of ZnS and ZnS:Mn^{2+} nanoparticles. ZnS nanoparticles showed an emission band at 457 nm ($\lambda_{exc.}$ = 319 nm) and ZnS:Mn^{2+} nanoparticle showed an emission band at 575 nm ($\lambda_{exc.}$ = 312 nm). ZnS:Mn^{2+} nanoparticle is ZnS semiconductor with manganese impurities. The orange emission of ZnS:Mn^{2+} nanoparticle is attributed to a $^4T_1 \rightarrow {}^6A_1$ transition of Mn^{2+} ion in T_d symmetry. The d-electron state of Mn^{2+} ion acts as efficient luminescent centers. Mn^{2+} ion has $3d^5$ configuration, which gives rise to a $^6S_{2/5}$ ground state in a tetrahedral crystal field. The first excited state of gaseous Mn^{2+} is ^4G. By the parity selection rule, the crystal-field (CF) transition is parity forbidden.[4] When Mn^{2+} ions are doped into the ZnS crystal, it replaces an amount of Zn^{2+}, and the ^4G of the first excited state of the Mn^{2+} in tetrahedral symmetry (T_d) has been split. Figure 16 show the energy levels of Mn d^5 configuration in T_d symmetry.[28][29] Because of the crystal-field disturbance, the effect of other ions around on electric structure of Mn^{2+} ion has relieved some forbidding. Then the crystal field transition of Mn^{2+} is strongly dependent on its host nanocrystal. The orange emission bands of ZnS:Mn^{2+} nanoparticle was attributed to the Mn^{2+} $^4T_1 \rightarrow {}^6A_1$ transition of the ZnS nanocrystal host.[30]

[31]

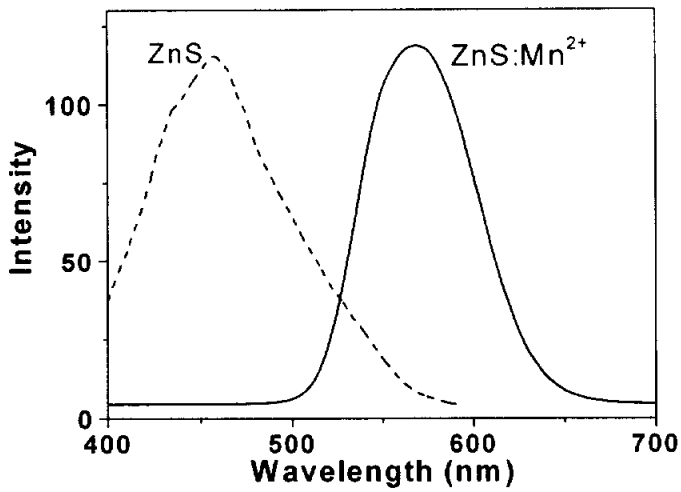

Figure 15. Emission spectra of ZnS and ZnS:Mn^{2+} nanoparticles

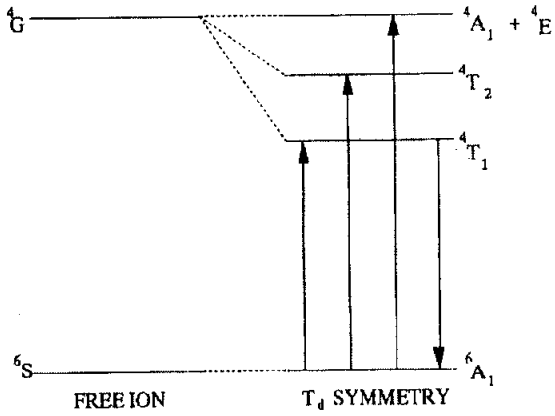

Figure 16. The energy levels of Mn d^5 configuration in T_d symmetry

4-2-3. Photoluminescence of ZnS:Mn^{2+} nanoparticle depending on the amount of Mn^{2+}

ZnS:Mn^{2+} nanoparticles are ZnS semiconductor crystal doped with manganese impurities. The orange-yellow emission is due to the d-d transition of Mn^{2+} ions. So, the emission intensity of ZnS:Mn^{2+} nanoparticle is dependent on the Mn^{2+} concentration in the ZnS lattice. The amount of Zn, S, Mn in the ZnS:Mn^{2+} nanoparticle was confirmed by TEM-EDX and the EDX spectra were shown in Figure 17. The amount of the Mn^{2+} in ZnS:Mn^{2+} nanoparticles was changed with the different concentrations of added $Mn(NO_3)_2$. The Mn^{2+} can substitute for Zn^{2+} ion in the ZnS crystal lattice because of their close ionic radii (0.80 and 0.83 Å for Mn^{2+} and Zn^{2+}, respectively).[36] So, the Mn/Zn atomic ratios of ZnS:Mn^{2+} I, ZnS:Mn^{2+} II and ZnS:Mn^{2+} III nanoparticles are shown in Table 2. Figure 18 shows the emission spectra of ZnS:Mn^{2+} nanoparticle with different amount of added Mn^{2+} nanoparticle. The Table 2 and Figure 18 show that the Mn^{2+} concentration in the ZnS increases and depends on the amount of Mn^{2+}.

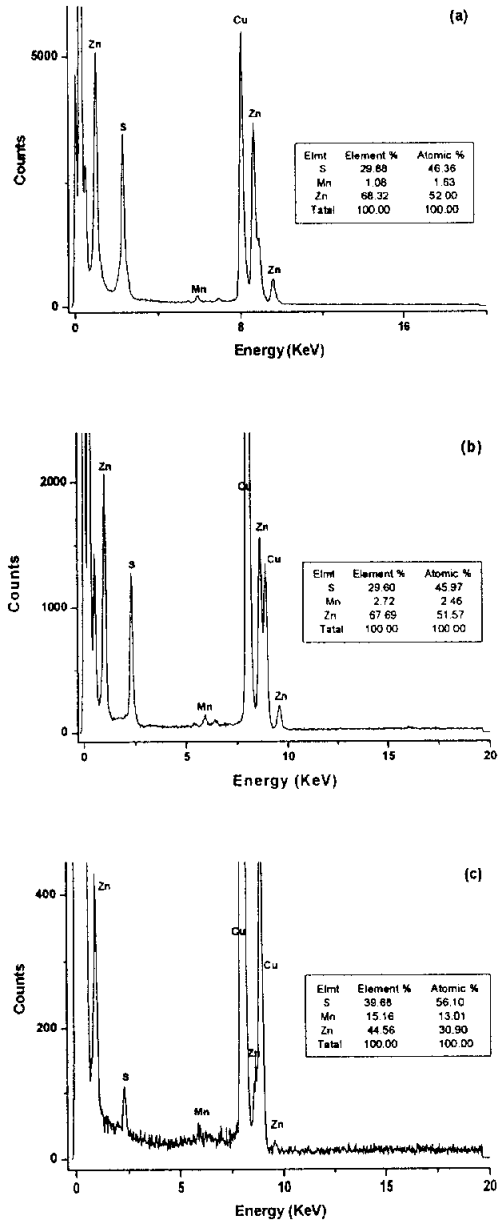

Figure 17. TEM-EDX of the $ZnS:Mn^{2+}$ I, $ZnS:Mn^{2+}$ II and $ZnS:Mn^{2+}$ III nanoparticles

Table 2. The Mn/Zn atomic ratios of ZnS:Mn^{2+} I, ZnS:Mn^{2+} II and ZnS:Mn^{2+} III nanoparticles

sample	Mn/Zn atomic ratio
ZnS:Mn^{2+} I	0.0313
ZnS:Mn^{2+} II	0.0477
ZnS:Mn^{2+} III	0.4210

The ZnS:Mn^{2+} III nanoparticle which have the largest amount of Mn^{2+} as Table 2 shows the largest emission intensity. But the ZnS:Mn^{2+} containing a lot of the Mn^{2+} ion always have not high emission intensity. The homogeneous distribution of Mn^{2+} ions in a ZnS crystal lattice is very important for the highly efficient luminescence.[30][31][32][33] For the inhomogeneous distribution of Mn^{2+} ions, local Mn^{2+}-Mn^{2+} pairs or clusters are formed in the ZnS crystals, which interact and lead to nonradiative relaxation under excitation. This results in low luminescence efficiency.[34][35]

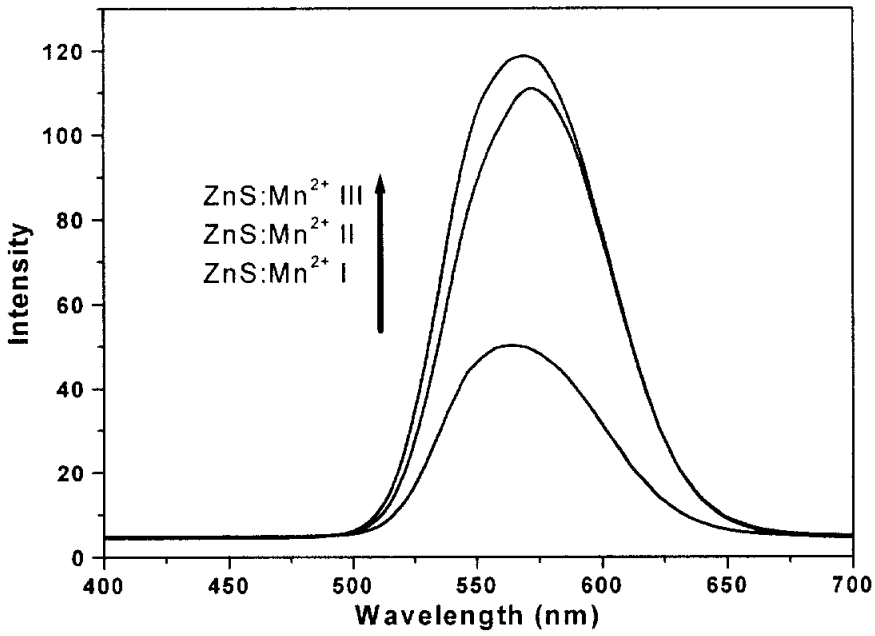

Figure 18. The emission spectra of $ZnS:Mn^{2+}$ nanoparticle with different amount of added Mn^{2+} nanoparticle

5. Summary

ZnO semiconductor nanoparticle having the n-type characteristic was prepared successfully by sol-gel method. Using the heat treatment, the size and particle shape were controlled. Also, the absorption and the emission band of ZnO nanoparticle shifted to blue with decreasing crystalline size when the size is sufficiently small. Also, the emission band at the visible range is due to defect related with deep level emissions, such as Zn interstitials or oxygen vacancies. ZnS and ZnS:Mn^{2+} nanoparticles were prepared by thermal annealing using auto-clave. By the auto-clave method, nanoparticles can be produced in large quantities. But the size and shape was irregular, since the particles were synthesized rapidly at high temperature and pressure with auto-clave. The emitting band of ZnS:Mn^{2+} nanoparticle showed red shift from that of ZnS nanoparticle and results in the emission band at 500 nm ~ 650 nm. The orange emission of ZnS:Mn^{2+} nanoparticle is attributed to a $^4T_1 \rightarrow {}^6A_1$ transition of Mn^{2+} ion in T_d symmetry. The emission intensity of ZnS:Mn^{2+} nanoparticle depends on the concentration of Mn^{2+} in the ZnS lattice. This optical property of semiconductor nanoparticles can be applied to photoconductor, transistors and sensor etc. Also they can be used to light wavelength modification.

6. References

[1] Srikant, V.; Clarke, D. R. *J. Appl. Phys.* **1998**, *83*, 5447

[2] King, S.; Gardeniers, J. G. E.; Boyd, I. W. *Appl. Surface Sci.* **1996**, 811, 96

[3] Rovvins, D. J.; DiMaria, D.J.; Falcony, C.; Dong, D. W. *J. Appl. Phys.* **1983**, 54, 4553

[4] Lee, E. C.; Kim, Y. S.; Jin, Y. G.; Chang, K. *J. Kor. phys. Soc.* **2001**, 39, S23

[5] Brus, L. *J. Phys. Chem. B* **1986**, 90, 2555

[6] Mach. R.; Mueller, G. O. *Phys. Status Solidi A* **1982**, 69, 11

[7] Bhargava, R. N.; Gallagher, D.; Hong, X.; Nurmikko, A. *phys. Rev. Lett.* **1994**, 72, 416

[8] Spanhel, L.; Anderson, M. A. *J. Am. Chem. Soc.* **1991**, *113*, 2826

[9] Meulenkanmp, E. A. *J. Phys. Chem. B* **1998**, 102, 5566

[10] Pesika, N. S.; Hu, Z.; Stebe, K. J.; Searson, P. C. *J. Phys. Chem. B* **2002**, 106, 6985

[11] C. Jeffrey binker, *Sol-Gel Science* **1990**

[12] Sumio, S. *Am. Ceram. Soc. Bull.* **1985**, 64, 1463

[13] Larry, L. H.; Jon, K.W. *Chem. Rev.* **1990**, 90, 33

[14] Lee, C.; Minyang, L.; Hyun, K. K.; Dae, W. M. *Bull. Korean, Chem. Soc.* **1997**, 18, 886

[15] Pacholski, C.; Kornowski, A.; Weller, H. *Angew. Chem. Int. Ed.* **2002**, *41*, 1188

[16] Swalin, R. A. "Thermodynamics of Solids", JOHN WILEY & SONS **1972**

[17] Azaroff, L. V. "Introduction to solids", McGRAW-HILL BOOK COMPANY, INC **1960**

[18] Studenikin, S.A.; Golego, N.; Cocivera, M. *J. Appl. Phys.* **1998**, 84, 2287

[19] Vanheusden, K.; Warren, W. L.; Seager, C. H.; Tallant, D. R.; Voigt, J. A.; Gnade, B. E. *J. Appl. Phys.* **1996**, 79, 7983.

[20] Kröger, F. A. The chemistry of imperfect crystals, NORTH-HOLLAND PUBLISHING COMPANY **1974**

[21] Egelhaaf, H. J.; OelKrug, D. *J. Crystal Growth* **1996**, 161, 190

[22] Lin, B.; Fu, Z.; Jia, y. *Appl. Phy. Lett.* **2001**, 79, 943

[23] Göpel, W. J. *Vacuum Science Technology* **1979**, 16, 1229

[24] Pfahml, A. *J. Electrochem. Soc.* **1962**, 109, 502

[25] Reynolds, D. C.; Look, D. C.; Jogai, B.; Litton, C. W.; Collins, T. C.; Harsch, W.; Cantwelll, G. *Phys. Rev. B* **1998**, 57, 12151

[26] Reynolds, D.C.; Look, D.C.; Jogai, B.; VanNostrrand, J. E.; Jones, R.; Jenny, *J. Solid State Communications* **1998**, 10, 701

[27] Reynolds, D. C.; Look, D. C.; Jogai, B.; Litton, C. W.; Collins, T. C.; Harsch, W.; Cantwelll, G. *J. Luminescence* **1999**, 82, 173

[28] Stavrev, K. K.; Nynev, K. D.; Nikolov, G. S. *J. Cryst. Growth* **1990**, 101, 376

[29] Pohl. U. W.; Busse, W. *J. Chem. Phys.* **1989**, 90, 6877

[30] Gan, L. M.; Liu, B.; Chew, C. H.; Xu, S. J.; Chua, S. J.; Loy, G. L.; Xu, G. Q. *Langmuir* **1997**, 13, 6427

[31] Yu, I.; Isobe, T.; Senna, M. *J. Phys. Chem. Solids* **1996**, 57, 373

[32] Hunter, A.; Kitai, A. H. *J. Appl. Phys.* **1987**, 62, 4244

[33] Yu, I.; Senna, M. *Appl. Phys. Lett.* **1995,** 66, 23

[34] Yang, H.; Wang, Z.; Song, L.; Zhao, M.; Chen, Y.; Dou, K.; Yu, J.; Wang, L. *Matt. Chem. Phys.* **1997**, 47, 249

[35] Lee, Y. H.; Ju, B. K.; Song, M. H.; Hahn, T. S.; Choh, S. H.; Oh, M. H. *J. Appl. Phys.* **1995**, 78, 4253

[36] Chen, W. *J. Appl. Phys.* **2000**, 88, 5188

[37] Kim, J. S.; Song, K. C.; Wilhelm, O.; Pratsinis, S. E. *Chemie ingenieur tech.* **2001**, 51, 461

[38] West, A. R. "Basic solid state chemistry", John Wiley & Sons, Ltd. **1988**

[39] Carter, R. L. "Molecular Symmetry and Group Theory ", John Wiley & Sons, Ltd. **1988**

[40] Bol. A.A; Meijerink, A. *J. Phys. Chem. B* **2001**, 105, 10197

[41] Xia, B.; Lenggoro, and Okuyama, K. *Chem. Master*. **2002**, 14, 4969

[42] Hench, L. L.; West, J. K. *Chem. Rev*. **1990**, 90, 33

7. Korean abstract

ZnO, ZnS는 넓은 band gap을 가진 반도체로써, 특정한 광학적 특성을 가진다. ZnO 나노입자는 zinc acetate가 포함된 에탄올 용액에 LiOH를 첨가하여 졸-겔 방법을 이용하여 합성하였다. ZnO 나노입자 크기는 열처리를 통해 조절하였다. ZnS와 ZnS:Mn^{2+} 나노입자는 각각 zinc oleate 용액과 $Mn(NO_3)_2$이 포함된 zinc oleate 용액에 Na_2S를 첨가하고, Auto-clave 방법을 이용하여 합성하였다. ZnO 광학적 특성을 입자크기에, ZnS:Mn^{2+}은 첨가한 Mn 양에 크게 의존한다. 나노입자의 크기는 TEM 이미지와 XRD의 반폭치로 계산하였으며 Mn^{2+}의 양은 TEM-EDX로 확인하였다.